

ChemComm

Accepted Manuscript



This is an *Accepted Manuscript*, which has been through the Royal Society of Chemistry peer review process and has been accepted for publication.

Accepted Manuscripts are published online shortly after acceptance, before technical editing, formatting and proof reading. Using this free service, authors can make their results available to the community, in citable form, before we publish the edited article. We will replace this *Accepted Manuscript* with the edited and formatted *Advance Article* as soon as it is available.

You can find more information about *Accepted Manuscripts* in the [Information for Authors](#).

Please note that technical editing may introduce minor changes to the text and/or graphics, which may alter content. The journal's standard [Terms & Conditions](#) and the [Ethical guidelines](#) still apply. In no event shall the Royal Society of Chemistry be held responsible for any errors or omissions in this *Accepted Manuscript* or any consequences arising from the use of any information it contains.



ChemComm

COMMUNICATION

Facile synthesis and surface chemistry of high quality wurtzite and kesterite $\text{Cu}_2\text{ZnSnS}_4$ nanocrystals using tin(II) 2-ethylhexanoate as a new tin source

Received 00th January 20xx,
Accepted 00th January 20xx

DOI: 10.1039/x0xx00000x

www.rsc.org/

Grzegorz Gabka,^a Piotr Bujak,^{a*} Maciej Gryszel,^a Andrzej Ostrowski,^a Karolina Malinowska,^b Grazyna Z. Zukowska,^a Fabio Agnese^{c,d}, Adam Pron^a and Peter Reiss^{c,e,f,**}

A novel synthesis method for $\text{Cu}_2\text{ZnSnS}_4$ nanocrystals is presented using a liquid precursor of tin, namely tin(II) 2-ethylhexanoate, which yields small and nearly monodisperse NCs either in the kesterite or in the wurtzite phase depending on the sulfur source (elemental sulfur in oleylamine vs. dodecanethiol).

$\text{Cu}_2\text{ZnSnS}_4$ (CZTS) quaternary semiconductor nanocrystals (NCs) have been drawing a significant research interest in the past few years as materials for solar¹ or thermal energy conversion to electricity.² Contrary to the NCs previously used for this purpose, they do not contain toxic (cadmium, lead) or rare (indium) elements. Their direct band gap which is close to the optimum value (~ 1.5 eV) and their high absorption coefficient ($\sim 10^4$ cm^{-1}) make them especially adequate for the use in solar cells.³ So far, for solar cells using CZTS-derived NCs, in particular mixed $\text{Cu}_2\text{ZnSnS}_x\text{Se}_{4-x}$ NCs of optimized band gap, the highest reported energy conversion efficiency amounted to 8.6%.⁴ In the case of thin films of $\text{Cu}_2\text{ZnSnS}_x\text{Se}_{4-x}$ deposited from hydrazine solutions of the precursors even higher efficiencies were measured, up to 12.6%.⁵

CZTS NCs have been mainly reported in two different crystallographic forms: tetragonal (kesterite) and hexagonal (wurtzite), the former being thermodynamically more stable.⁶ High temperature syntheses with the use of simple metal salts in combination with elemental sulfur in oleylamine (OLA) as the solvent yield NCs of the kesterite structure.^{2,7} Alternatively, metal salts and sulfur can be replaced by one-component precursors, namely metal dithiocarbamate complexes.⁸

Metastable wurtzite-type CZTS NCs can be obtained from

very similar metal precursors⁹ and also from metal dithiocarbamate complexes,^{8c} however, the addition of alkanethiols as a source of sulfur is necessary in this case. Both kesterite- or wurtzite-type CZTS NCs can also be prepared in a controllable manner by varying the reactivity of the sulfur precursor.¹⁰ Injection of the solution of higher reactivity (prepared by heating *S*/octadecene (ODE) for 2 hrs at 155°C) leads to NCs of wurtzite-type structure while the less reactive sulfur precursor solution (obtained by heating the sulfur solution 1 hr) yields kesterite NCs. The opposite is observed if the synthesis of NCs is carried out in OLA: the use of a highly reactive precursor solution, namely sulfur dissolved in OLA, results in kesterite NCs whereas a less reactive 1-dodecanethiol (DDT)/OLA precursor solution produces wurtzite ones.¹¹ These two examples unequivocally show that the reactivity of the sulfur precursor cannot play a predictive role as far as the crystallographic structure of the resulting CZTS NCs is concerned. The *hot-injection* method provides a versatile approach for the temporal separation of nucleation and growth of NCs, leading to narrow size dispersion. However, a drawback of this method is the limited availability of metal precursors, which could easily be dissolved at room temperature. Therefore, generally only the chalcogenide precursors are injected. In the case of multinary NCs the ability to inject also the metal precursors would give the opportunity to reduce the formation of secondary phases during the temperature increase of the reaction mixture.

In this communication we report a novel synthesis of CZTS NCs, in which we replace solid and difficult to dissolve precursors of tin by liquid tin(II) 2-ethylhexanoate. This compound, never previously used in nanocrystal synthesis, is a popular catalyst for polymerization of L-lactide.¹² Application of this new tin precursor in combination with the appropriate sulfur precursor (DDT or DDT+S/OLA) and reaction conditions (heating up vs. hot injection) allows for a strict control of the NCs' structure and size. Finally, we demonstrate by means of NMR spectroscopy that the obtained wurtzite and kesterite CZTS nanocrystals exhibit distinct differences in the nature of their surface capping ligands.

^a Faculty of Chemistry, Warsaw University of Technology, Noakowskiego 3, 00-664 Warsaw, Poland, E-mail: piotr.bujakchem@poczta.onet.pl.

^b Faculty of Chemistry, University of Warsaw, Pasteura 1, 02-093 Warsaw, Poland.

^c Univ. Grenoble Alpes, 38000 Grenoble, France. ^d CEA-INAC-SP2M, Laboratoire d'Etude des Matériaux par Microscopie Avancée. ^e CEA-INAC-SPRAM, Laboratoire d'Electronique Moléculaire, Organique et Hybrid, 17 rue des Martyrs, 38054 Grenoble cedex 9, France. ^f CNRS UMR5819 SPRAM, 38000 Grenoble, France, E-mail: peter.reiss@cea.fr.

† Electronic Supplementary Information (ESI) available: Experimental details, Raman, UV-vis, EDS, NMR, MS spectra, TEM images, band-gap energy calculation. See DOI: 10.1039/x0xx00000x

Table 1 Reaction parameters and characteristics of the synthesized CZTS nanoparticles.[§]

Sample	Type	Solvent	Sulfur source	Size (nm)	Composition	Structure
CZTS-1	HU	ODE	DDT	6.0 +/-2.0	Cu _{2.04} Zn _{1.00} Sn _{1.37} S _{4.76}	Wurtzite
CZTS-2	HI	ODE	DDT+ S/OLA	3.4 +/-0.7	Cu _{1.94} Zn _{1.00} Sn _{0.92} S _{3.81}	Kesterite
CZTS-3	HI	ODE	S/OLA	5-18	Cu _{1.41} Zn _{1.00} Sn _{0.72} S _{3.14}	Kesterite
CZTS-4	HI	DCB	DDT+ S/OLA	3.0 +/-0.9	Cu _{2.10} Zn _{1.00} Sn _{0.92} S _{3.89}	Kesterite

[§] HU: heating-up; HI: hot-injection; ODE: 1-octadecene; DCB: 1,2-dichlorobenzene; DDT: 1-dodecanethiol; OLA: oleylamine.

In all syntheses the new precursor was used in combination with copper(II) oleate and zinc acetate as precursors of metals. Commercially available tin(II) 2-ethylhexanoate is a liquid stable in air, which readily mixes with commonly used solvents like ODE or OLA. This new set of metal precursors was tested in the two most popular CZTS NCs synthesis methods, namely *heating-up* and *hot-injection*. **Table 1** gives an overview of the synthetic parameters and characteristics of the obtained samples.

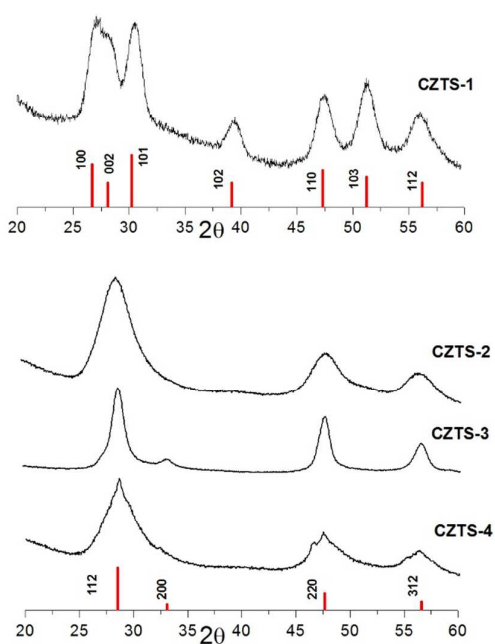


Fig. 1 X-ray diffractograms of the different samples. CZTS-1: red bars indicate the diffraction pattern of wurtzite CZTS^{9a,11}; CZTS-2/3/4: the peak positions of bulk kesterite CZTS are indicated (JCPDS 26-0575).

The *heating-up* method (230 °C, 3h) with the use of the above described set of metal precursors and DDT in ODE as the sulfur precursor led to hexagonal (wurtzite) CZTS NCs (denoted as **CZTS-1**), as evidenced by the diffractogram shown in **Fig. 1**.^{9a,11} Raman spectroscopy is a very sensitive tool for investigation of the phase purity of CZTS NCs. In particular, even small amounts of ZnS, undetectable in powder diffractograms, give rise to Raman bands at higher wavenumbers as compared to the characteristic diagnostic band of kesterite at 331 cm⁻¹ (see **Fig. S1** in ESI[†]).^{9b} The

composition of the obtained NCs was Cu_{2.04}Zn_{1.00}Sn_{1.37}S_{4.76} as determined by EDS (see **Fig. S4** ESI[†] for the corresponding spectrum). Their small size should be pointed out, 6.0 +/-2.0 nm (see **Fig. 2** and **Fig. S2** ESI[†]). Along with nanoparticles described in Ref. 9, they are the smallest wurtzite-type CZTS NCs reported to date.

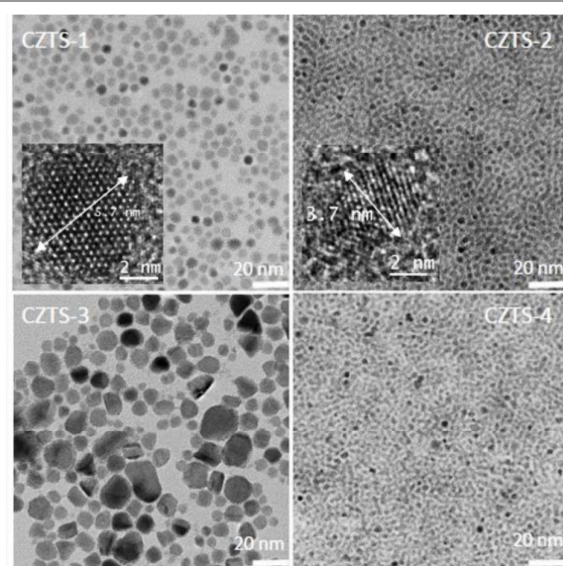


Fig. 2 TEM images of the different samples at identical magnification and HRTEM images of wurtzite-CZTS-1 and kesterite-CZTS-2 NCs.

The same set of precursors was also tested in the *hot-injection* method of the CZTS NCs preparation. In this procedure a mixed solution of sulfur and tin(II) 2-ethylhexanoate in OLA were injected into a mixture of copper(II) oleate, zinc acetate and DDT in ODE heated to 170 °C. Then the temperature was raised to 230 °C and kept at this temperature for additional 30 minutes. The resulting NCs (**CZTS-2**) of the almost "ideal" 2:1:1:4 composition Cu_{1.94}Zn_{1.0}Sn_{0.92}S_{3.81} and 3.4 +/-0.7 nm size were essentially monodisperse (see **Fig. 2**) and exhibited the kesterite structure (JCPDS No. 26-0575) (**Fig. 1**). In this synthesis two sulfur sources were used, namely DDT and elemental sulfur in OLA. To identify the role of both precursors we performed an additional synthesis without DDT. This procedure led to NCs in the kesterite structure (**CZTS-3**, **Fig. 1**) having a composition of Cu_{1.41}Zn_{1.00}Sn_{0.72}S_{3.14}. They were much bigger and more polydisperse than those of the **CZTS-2** batch, showing a

diameter in a size range of 5 - 18 nm (Fig.2). CZTS-4 was prepared using the same parameters as for CZTS-2 but with 1,2-dichlorobenzene instead of ODE as the solvent (*vide infra*).

To summarize this synthetic part of the paper, NCs of wurtzite structure (CZTS-1) are obtained with DDT as the only source of sulfur in a heating-up synthesis. The reaction likely proceeds *via* binary and ternary wurtzite-type Cu-S and Cu-Zn-S phases, favoring this crystal structure in the final product.¹⁰ In the case of the kesterite-type NCs CZTS-2 and CZTS-4, DDT serves for the complexation of the Cu and Zn precursors in ODE, while the actual predominant sulfur source in this case is S/OLA. This can be judged from the observed color changes. With only DDT temperatures of at least 180-200°C are required for observing a gradual color change from orange to black indicative of NC formation. When injecting S/OLA together with the tin precursor at 170°C (CZTS-2, CZTS-4), the reaction mixture immediately turns black. However, also in this type of reaction DDT plays a crucial role as it intervenes in the formation of intermediate precursor complexes and the control of the reaction kinetics. Its absence in the reaction mixture results in the formation of larger NCs of higher polydispersity (CZTS-3). More detailed studies of the reaction mechanism are currently undertaken.

In our recent paper we have described an efficient method for the identification of NCs' surface ligands based on NMR studies of organic molecules recovered after the dissolution of the inorganic cores.¹³ This procedure provides more precise information concerning the organic shell than direct studies of organic ligands capped NCs since their NMR spectra suffer from line broadening caused by the limited mobility of the surface-bound molecules. Detailed description of the applied ligands recovery procedure can be found in ESI[†]. As seen from the ¹H NMR spectrum shown in Fig. 3, for CZTS-1 (wurtzite) DDT molecules were recovered, playing a dual role as the sulfur precursor and capping ligand. Additionally, lines attributable to oleic acid (OA) (the second expected ligand) and to ODE (solvent) could be distinguished.

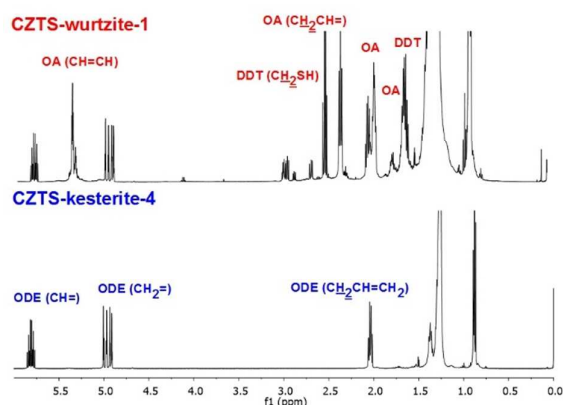


Fig. 3 ¹H NMR spectra of the NCs' surface ligands recovered after dissolution of the inorganic cores. Top: CZTS-1 (wurtzite); bottom: CZTS-4 (kesterite).

To the contrary, ¹H NMR spectra of the ligands recovered through the inorganic core dissolution of CZTS-2 indicated ODE as essentially the sole organic molecule. No lines attributable to DDT and oleic acid, clearly observed in the spectra of CZTS-1, could be detected in this case. To verify whether the recovered ODE originated from the solvent or alternatively from the chemical transformation of other molecules present in the reaction mixture, we carried out an additional synthesis of CZTS NCs, in which ODE was replaced by 1,2-dichlorobenzene as the solvent. In this case a solution of sulfur and tin(II) 2-ethylhexanoate in OLA was injected into a solution of copper(II) oleate and zinc acetate in dichlorobenzene, previously heated to 150 °C. The temperature was then raised to 180 °C and kept constant for additional 1 hour. Since 180 °C is the boiling point of dichlorobenzene, the heat exchange is very effective with no necessity of applying a strict temperature regime. In these conditions essentially monodisperse kesterite NCs of small size (3.0 +/-0.9 nm) formed, showing a composition of Cu_{2.16}Zn_{1.00}Sn_{0.92}S_{3.89} (see CZTS-4 in Fig. 1 and 2). Note that in this case a small admixture of the anilite (Cu₇S₄) phase is observed in addition to the kesterite phase. It is evidenced by two reflections of very low intensity at 46.4° and 32,3° unequivocally ascribed to anilite (JCPDS 22-0250).¹⁴ Both the size and composition are almost identical with the values obtained from the synthesis in ODE (CZTS-2), indicating at a first glance that the choice of the solvent did not significantly influence the reaction mechanism. Raman spectroscopy (see Fig. S1 in ESI[†]) revealed the presence of the pure kesterite structure with a peak at 333 cm⁻¹, unequivocally excluding the presence of a mixture of phases such as Cu₂SnS₃ and ZnS.¹⁵

In Fig. 3 the ¹H NMR spectrum of the ligands recovered from CZTS-4 is compared with the corresponding spectrum of the CZTS-1 ligands. To facilitate the attribution ¹H NMR spectra of free ODE, DDT, OLA and oleic acid are collected in Fig. S5 (ESI[†]). Surprisingly, distinct signals of ODE were present in the ¹H NMR of the ligands recovered from CZTS-4 NCs, despite the fact that no ODE was used at any step of their preparation. The presence of ODE in the recovered organic part of the NCs was additionally confirmed by GC-MS whose spectrum unequivocally indicated the presence of ODE (Fig. S6, ESI[†]). No evidence of DDT and oleic acid could be found, similarly as in the case of the other two kesterite-type NCs studied (CZTS-2 and CZTS-3). It is therefore clear that ODE had to be formed from OLA or oleic acid either in the course of NCs' synthesis or during the process of the inorganic core dissolution and ligands recovery. The formation of 1-alkene from OLA must proceed *via* an elimination reaction accompanied by hydrogenation. This type of elimination reaction has been reported when heating fcc Co nanoparticles with OLA to > 200 °C.¹⁶ In our case a possible reaction mechanism comprises i) bond formation between a surface metal atom and a carbon atom of the α-CH₂ group of OLA; ii) cleavage of the C-N bond in this complex under simultaneous formation of 1-alkene via β-H elimination, affording ODE

and eventually other side-products like octadecadiene, heptadecene and heptadecadiene.

The optical band gap of **CZTS-4** (kesterite), was determined on the basis of UV-vis absorption spectroscopy as 1.65 eV (see Fig. S7, ESI[†]). The slightly increased value as compared to the values calculated theoretically (1.56 eV) and measured experimentally (1.4–1.6 eV) for bulk kesterite¹⁷ could be indicative of quantum confinement effects. The Bohr exciton radius of kesterite, calculated on the basis of available literature data,¹⁶ is rather small (in the range of 2.2 to 3.4 nm, depending on assumptions used for the calculations), hence NCs of 3.0 +/-0.9 nm size, described here should reveal quantum confinement, as observed experimentally.

In the UV-vis-NIR spectrum of the wurtzite-type NCs **CZTS-1** (Fig. S7, ESI[†]) no broad absorption band in the NIR spectral range was observed. This can be taken as an additional proof of phase purity since the NIR band has been attributed to the heterophase system Cu_{1.92}S-CZTS.^{9d} We have determined the optical band gap to be 1.75 eV, *i.e.* significantly higher than the value reported for wurtzite-type CZTS NCs (1.4–1.5 eV).⁹ It should be however noted that the literature values were measured for nanoparticles exceeding 20 nm in size, whereas the NCs reported here are much smaller (6.0 +/-2.0 nm). Furthermore, band gap variation arising from deviation from the 2:1:1:4 stoichiometry is not taken into account.

Conclusions

To summarize, we have presented a new method for the phase-controlled synthesis of small sized CZTS NCs of narrow size distribution through the introduction of the new tin precursor tin(II) 2-ethylhexanoate. Used in a heating-up method with DDT as the sulfur source, it leads to wurtzite-type NCs, while a hot-injection method using the same set of precursors but S/OLA as the sulfur source yields NCs in the kesterite phase. The two types of CZTS NCs exhibit distinct differences in surface chemistry involving ligand transformation in the case of the kesterite NCs. An increased optical band gap with respect to literature data for bulk kesterite CZTS is observed, indicative of quantum confinement effects. The fine-control of the composition, crystal structure and band gap allow for the study of the influence of these parameters on the properties of optoelectronic devices using CZTS NCs, enabling optimization of their performance.

This research was carried out in the framework of the project entitled "New solution processable organic and hybrid (organic/inorganic) functional materials for electronics, optoelectronics and spintronics" (Contract No. TEAM/2011-8/6), which is operated within the Foundation for the Polish Science Team Programme cofinanced by the EU European Regional Development Fund. One of the authors (P.B.) wants to acknowledge a partial financial support of the Warsaw University of Technology. The TEM

images were obtained using the equipment purchased within CePT Project No. POIG.02.02.00-14-024/08-00.

Notes and references

- (a) K. Ramasamy, M. A. Malik, P. O'Brien, *Chem. Commun.*, 2012, **48**, 5703; (b) S. Chen, A. Walsh, X.-G. Gong, S.-H. Wei, *Adv. Mater.*, 2013, **25**, 1522; (c) U. Ghorpade, M. Suryawanshi, S. W. Shin, K. Gurav, P. Patil, S. Pawar, C. W. Hong, J. H. Kim, S. Kolekar, *Chem. Commun.*, 2014, **50**, 11258.
- H. Yang, L. A. Jauregui, G. Zhang, Y. P. Chen, Y. Wu, *Nano Lett.*, 2012, **12**, 540.
- (a) H. Katagiri, K. Jimbo, W. S. Maw, K. Oishi, M. Yamazaki, H. Araki, A. Takeuchi, *Thin Solid Films*, 2009, **517**, 2455; (b) S. Siebentritt, S. Schorr, *Prog. Photovolt. Res. Appl.*, 2012, **20**, 512.
- W.-C. Hsu, H. Zhou, S. Luo, T.-B. Song, Y.-T. Hsieh, H.-S. Duan, S. Ye, W. Yang, C.-J. Hsu, C. Jiang, B. Bob, Y. Yang, *ACS Nano*, 2014, **8**, 9164.
- W. Wang, M. T. Winkler, O. Gunawan, T. Gokmen, T. K. Todorov, Y. Zhu, D. B. Mitzi, *Adv. Energy Mater.*, 2014, **4**, 1301465.
- D. Aldakov, A. Lefrançois, P. Reiss, *J. Mater. Chem. C*, 2013, **1**, 3756.
- (a) T. Kameyama, T. Osaki, K.-ichi. Okazaki, T. Shibayama, A. Kudo, S. Kuwabata, T. Torimoto, *J. Mater. Chem.*, 2010, **20**, 5319; (b) T. Rath, W. Haas, A. Pein, R. Saf, E. Maier, B. Kunert, F. Hofer, R. Resel, G. Trimmel, *Sol. Energy Mater. Sol. Cells*, 2012, **101**, 87; (c) A. Shavel, D. Cadavid, M. Ibáñez, A. Carrete, A. Cabot, *J. Am. Chem. Soc.*, 2012, **134**, 1438.
- (a) C. Zou, L. Zhang, D. Lin, Y. Yang, Q. Li, X. Xu, X. Chen, S. Huang, *CrystEngComm*, 2011, **13**, 3310; (b) A. Khare, A. W. Wills, L. M. Ammerman, D. J. Norris, E. S. Aydil, *Chem. Commun.*, 2011, **47**, 11721; (c) M. D. Regulacio, C. Ye, S. H. Lim, M. Bosman, E. Ye, S. Chen, Q.-H. Xu, M.-Y. Han, *Chem. Eur. J.*, 2012, **18**, 3127.
- (a) X. Lu, Z. Zhuang, Q. Peng, Y. Li, *Chem. Commun.*, 2011, **47**, 3141; (b) A. Singh, H. Geaney, F. Laffir, K. M. Ryan, *J. Am. Chem. Soc.*, 2012, **134**, 2910; (c) M. Li, W.-H. Zhou, J. Guo, Y.-L. Zhou, Z.-L. Hou, J. Jiao, Z.-J. Zhou, Z.-L. Du, S.-X. Wu, *J. Phys. Chem. C*, 2012, **116**, 26507; (d) H.-C. Liao, M.-H. Jao, J.-J. Shyue, Y.-F. Chen, W.-F. Su, *J. Mater. Chem. A*, 2013, **1**, 337; (e) J. Chang, E. R. Waclawik, *CrystEngComm*, 2013, **15**, 5612.
- Y. Zou, X. Su, J. Jiang, *J. Am. Chem. Soc.*, 2013, **135**, 18377.
- Z. Li, A. L. K. Lui, K. H. Lam, L. Xi, Y. M. Lam, *Inorg. Chem.*, 2014, **53**, 10874.
- R. E. Drumright, P. R. Gruber, D. E. Henton, *Adv. Mater.*, 2000, **12**, 1841.
- G. Gabka, P. Bujak, M. Gryszel, K. Kotwica, A. Pron, *J. Phys. Chem. C*, 2015, **119**, 9656.
- V. T. Tiong, Y. Zhang, J. Bell, H. Wang, *CrystEngComm.*, 2014, **16**, 4306.
- P. A. Fernandes, P. M. P. Salomé, A. F. da Cunha, *J. Alloys Compd.*, 2011, **509**, 7600-7606.
- (a) K. M. Nam, J. H. Shim, H. Ki, S.-I. Choi, G. Lee, J. K. Jang, Y. Jo, M.-H. Jung, H. Song, J. T. Park, *Angew. Chem. Int. Ed.*, 2008, **47**, 9504; (b) S. Mourdikoudis, L. M. Liz-Marzán, *Chem. Mater.*, 2013, **25**, 1465.
- C. Persson, *J. Appl. Phys.*, 2010, **107**, 053710.

